SUPPLEMENTARY METHODS

Fourier analysis: The Fourier transform of the fMRI time series at a voxel at the stimulus frequency (here 8 cycles/run) yields a vector with real and imaginary components, or the amplitude and the phase. For a polar angle mapping scan, the phase of this vector corresponds to the polar angle of the preferred stimulus location. The amplitude reflects the strength of the retinotopic response and is equal to -log10 of the *p*-value (e.g. -log10(0.0001) = 4). The significance is estimated by dividing the squared amplitude of the signal at the stimulus frequency by the sum of squared amplitudes at all other frequencies ("noise" frequencies), excluding low frequencies, and harmonics of the stimulus frequency (Sereno et al. 1995). This is a ratio of two χ^2 statistics and has an *F*-distribution (Larsen and Marx 1986) and thus a corresponding statistical *p*-value can be obtained (degrees of freedom being the number of time points). Note that this significance estimate is actually conservative because the "noise" we are dividing by in this case is not evenly distributed across frequencies.

The phase of the signal at the stimulus frequency denotes retinotopic coordinates (here, polar angle). In standard fMRI analyses, pseudocolor scales are typically used to represent the amplitude of the response (often after masking the data with a significance threshold). Similarly, in phase-encoded mapping studies, pseudocolor is used in order to represent the phase of the response – but the saturation of the color is modulated as a function of the signal amplitude using a sigmoid function. The sigmoid function can be set such that the visibly saturated phase colors begin to emerge from the background at a chosen threshold, leading to a result similar to a standard fMRI analysis. This procedure has been used in many previous studies (e.g., Tootell et al. 1997). In our group data figures (Figs 2-4), the sigmoid function was set so that phase colors begin to emerge at $p < 10^{-3}$. However, the data at most the activated cortical surface points has much higher significance values ($p < 10^{-5}$ to $p < 10^{-10}$).

A similar analysis was used to distinguish between positive- and negative-going MR signal fluctuations in the case of two-condition stimulus comparisons (ANOVA analyses, Figs. 5,6).

Vector averaging: To increase signal to noise, multiple scans are averaged in the Fourier domain. The real and imaginary components are averaged across scans independently. Vector averaging penalizes voxels with inconsistent phase and rewards voxels with consistent phase: If the phases of the Fourier transform at a frequency are varying randomly, the amplitude of a vector average will tend towards zero. Voxels at which the Fourier transform has high amplitude *and* consistent phase across runs will have the maximal ratio between stimulus and noise frequencies.

Each subject was scanned with an equal number of scans with counterclockwise or clockwise stimulus revolutions in order to guarantee that any phase-spread in the results is not due to local static differences in hemodynamic delay. Phases for clockwise data were reversed before averaging and 0.06 cycles of phase were subtracted from the data before averaging to offset the hemodynamic delay (Sereno et al., 1995). Ipsilateral phases were truncated after averaging. This only affected a handful of voxels per scan.

Group Averaging: The group data were analyzed using spherical surface-based methods using FreeSurfer (Dale et al. 1999; Fischl et al. 1999a; Fischl et al. 1999b). To perform spherical averaging, each subject's cortical surface was reconstructed and then morphed to an average spherical representation of the cerebral hemispheres that optimally aligns the sulcal and gyral features across subjects, through a procedure that aims to match these features across subjects while minimizing metric distortion (Fischl et al., 1999b). Each subject's functional data were first interpolated onto the spherical representation of their hemispheres using FreeSurfer. Then these data were morphed and resampled onto the common spherical space.

For surface-based group analyses of the complex data, spherical averaging of the amplitude and phase are carried out separately. For ANOVA analyses, amplitude was set positive or negative depending

on whether the phase represented contralateral or ipsilateral space. A two-factor ANOVA was performed using a mixed-effects model, with condition as the fixed effect and subjects as the random effect. 16 steps of iterative spatial smoothing on the spherical surface were applied to the data (corresponding to a Gaussian filter with a full-width at half-maximum of approximately 4 mm, along the cortical surface – Hagler et al. 2006) before conducting group statistics using AFNI (Cox 1996). The resulting statistics were then transferred onto the inflated cortical surface of a single subject for display (Figures 2 – 4 and S1, S2).

References

Cox RW. 1996. AFNI: software for analysis and visualization of functional magnetic resonance neuroimages. Comput Biomed Res. 29(3): 162-173.

Dale AM, Fischl B, Sereno MI. 1999. Cortical surface-based analysis. I. Segmentation and surface reconstruction. Neuroimage. 9(2): 179-194.

Fischl B, Sereno MI, Dale AM. 1999a. Cortical surface-based analysis. II: Inflation, flattening, and a surface-based coordinate system. Neuroimage. 9(2): 195-207.

Fischl B, Sereno MI, Tootell RB, Dale AM. 1999b. High-resolution intersubject averaging and a coordinate system for the cortical surface. Hum Brain Mapp. 8(4): 272-284.

Hagler DJ, Jr., Saygin AP, Sereno MI. 2006. Smoothing and cluster thresholding for cortical surface-based group analysis of fMRI data. Neuroimage. 33(4):1093-103.

Larsen RJ, Marx ML. 1986. An Introduction to Mathematical Statistics and Its Applications. Englewood Cliffs, New Jersey: Prentice-Hall.

Sereno MI, Dale AM, Reppas JB, Kwong KK, Belliveau JW et al. 1995. Borders of multiple visual areas in humans revealed by functional magnetic resonance imaging. Science. 268(5212): 889-893.

Tootell RB, Mendola JD, Hadjikhani NK, Ledden PJ, Liu AK et al. 1997. Functional analysis of V3A and related areas in human visual cortex. J Neurosci. 17(18): 7060-7078.

Supplementary Figure 2. Variant of the Attention condition. In an additional experiment, Subject 3 was scanned in the Attention condition, keeping track of the rotating wedge without a color cue (see Results). Visibly saturated phase colors emerge at $p < 10^{-5}$. The results closely resembled those obtained using the color cue, showing that these regions are driven by attention and not by the color cue per se.

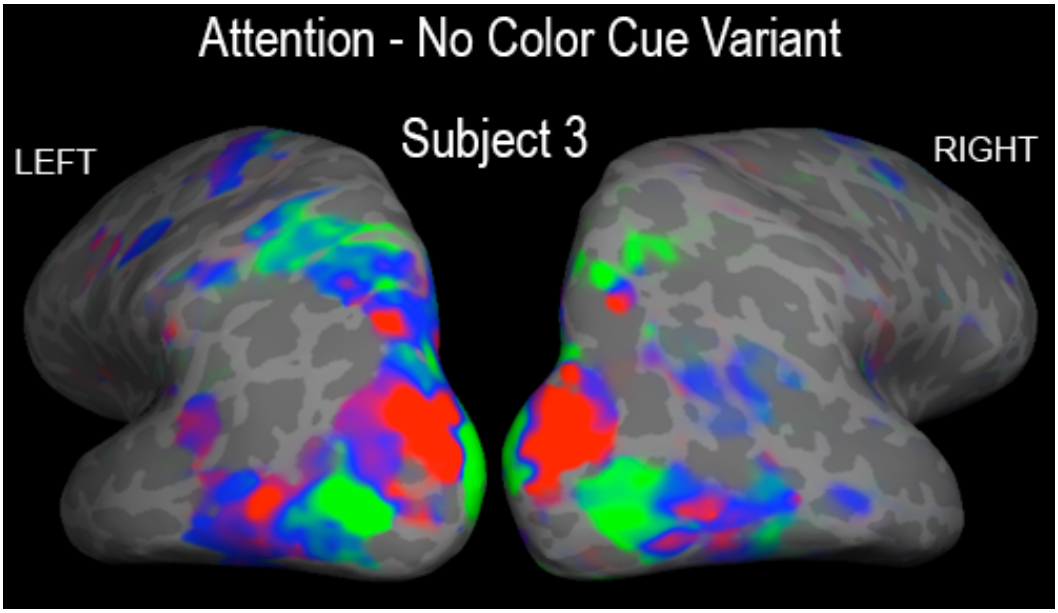

Supplementary Figure 3. Retinotopic responses in relation to regions sensitive to biological motion. Significant activity revealed in the main experiment is shown overlaid with areas of the human brain known to be sensitive to point-light biological motion. The map shown here is identical to Figure 2a. The white outlines depict boundaries of the regions that were most responsive to the specific contrast of biological motion to scrambled biological motion as mapped in a block design group study by Saygin et al. (J. Neurosci. 2004). The biological motion and scrambled motion stimuli used in the block design mapping study were identical to those used in the retinotopic stimuli in the present experiments. Lateral temporal cortical areas that are sensitive to biological motion have notable overlap with the retinotopic responses in the present study. The frontal areas that are most sensitive to biological motion however, are distinct from the most significant frontal maps we obtained, which are in the FEF. Note that when compared to a less subtle control stimulus, biological motion activates a more expansive region, which overlaps more of the retinotopic extent than shown here (see Saygin et al. 2004).

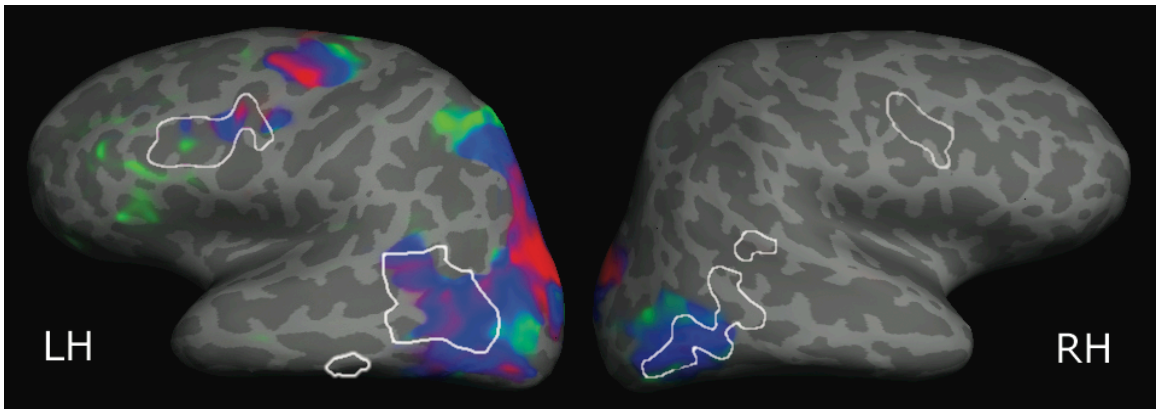

SUPPLEMENTARY DATA

Part 1: ANOVA

To explore the differences between conditions more quantitatively, we performed voxel-by-voxel analyses of variance (ANOVA) with subjects as random effects. Here, the comparison of the Attention+Stimulus and Stimulus conditions results in an Attention effect; the comparison of the Attention+Stimulus and Attention conditions results in a Stimulus effect.

Attention effect (Attention+Stimulus – Stimulus)

Attention increased retinotopic activity in most areas in which maps were found (Figs. S1a-c). Overall, attention effects were stronger in the right hemisphere – this is due to the right hemisphere showing a stronger reduction in activity compared with the left hemisphere when attention was not directed to the retinotopic stimuli (see Figs. 2b, 3b and Supplementary Fig. 1).

There were highly significant Attention effects in posterior parietal cortex (especially in the right hemisphere) and the FEF; these were expected given that these regions were not strongly activated in in the absence of directed attention. Additionally, some areas that did respond in the Stimulus condition also showed significant attentional modulation, such as portions of lateral temporal cortex (stronger in the right hemisphere, Fig. 3a-b, S1a-b), LIP/IPS1 (left hemisphere, Fig. 3b, S1b), and additional ventral and dorsal visual areas (Figs. 3c, S1c, 3d, S1d).

In contrast to the significant differences found in higher areas, primary visual cortex (V1 and most of V2) did not show a strong Attention effect (medial view, Figure S1d). Significant attention effects began higher along the visual processing stream: in peripheral V2, V3, VP, V4v+V8/hV4+VO (Fig. S1c), V3A, V7 (Fig. S1b), and V6 (Fig. S1d).

Stimulus effect (Attention+Stimulus – Attention)

As expected based on the extreme similarity of the responses we observed for the Attention+Stimulus and

Attention conditions in higher areas, the Stimulus contrast was found in mainly in early areas V1, V2, V3, VP, and V3A (Fig. S2). Additional stimulus-sensitive areas included a small portion of LOC, a small area anterior to MT, and a small fusiform area (Fig. S2 b,c).

Part 2: Non-biological Structured Motion Stimuli

On a small number of subjects, we ran a variant of the Attention+Stimulus condition in which non-biological motion was used as stimuli. The task and design were the same as those described in the Attention+Stimulus condition of the main study. The stimulus display was also similar to the other studies: We used "objects" or "scrambled objects" made up of point-lights, but these objects moved non-biologically. Each object contained the same number (12) and size of point-lights as the biological motion stimuli. Three copies of a shape were presented in the wedge. The objects carried out a translating motion achieved by all dots moving uniformly in one of eight directions (up, down, sideways, diagonal). This point-light object is also an example of structured motion but the motion is not biological. In the background, we presented spatially scrambled versions of the same dots. This scrambling disrupts global form as in scrambled biological motion. Subjects had to fixate and keep their attention on the wedge. They responded when not all three shapes moved in the same direction. This task is also difficult and requires attention to perform successfully. Thus, the experiment corresponded to the Attention+Stimulus condition of the main study.

While a definitive conclusion cannot be made without conducting a larger study, activation sevoked by this variant of the experiment were qualitatively very similar to the ones found in the main experiment where the stimulus display contained biological motion animations. Subject 3's results are included here (Fig S3).

The retinotopic activity we identified may be largely unspecific to biological motion; at least they appear to also be driven by other structured motion stimuli. This result is perhaps not unexpected given the large attention effects and relatively small or non-existent stimulus effects we found in most areas.

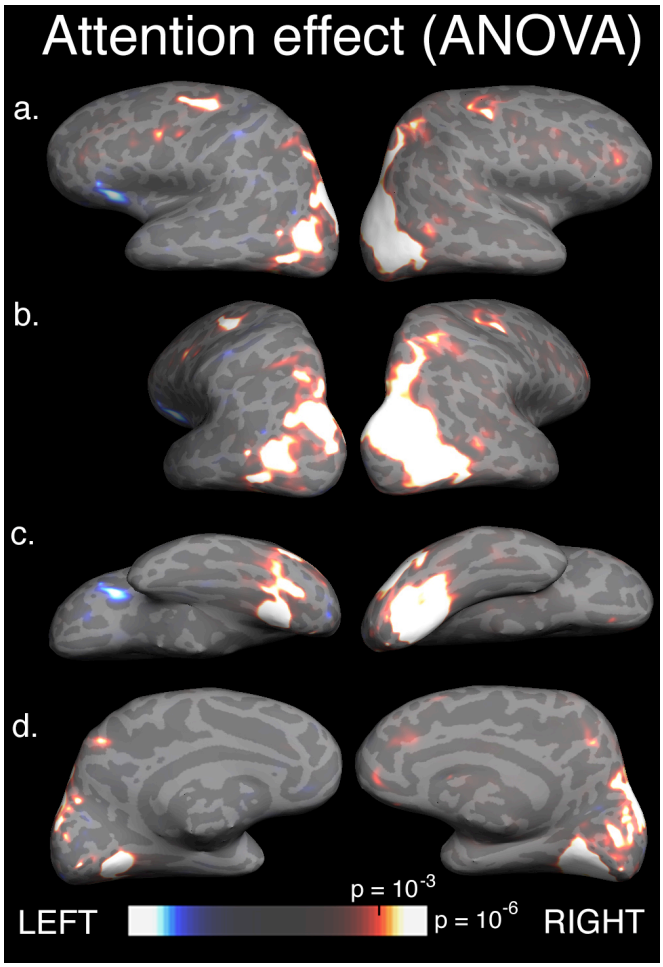

Figure S1. Surface-based group average: Attention effect. Here we contrast the Attention + Stimulus condition and the Stimulus conditions to quantitatively show areas which show significant attentional modulation. At each voxel, an ANOVA is carried out using the amplitude of the Fourier transform on the spherical surface with subjects (n=9) as random effect (see Methods). Results are displayed on the lateral (a), dorsolateral (b), ventral (c) and medial (d) views of a single subject's inflated cortical hemispheres. Visibly saturated phase colors begin to emerge at $p < 10^{-3}$, where red-yellow-white coloring range represents the Attention effect (see Methods, Supplementary Methods).

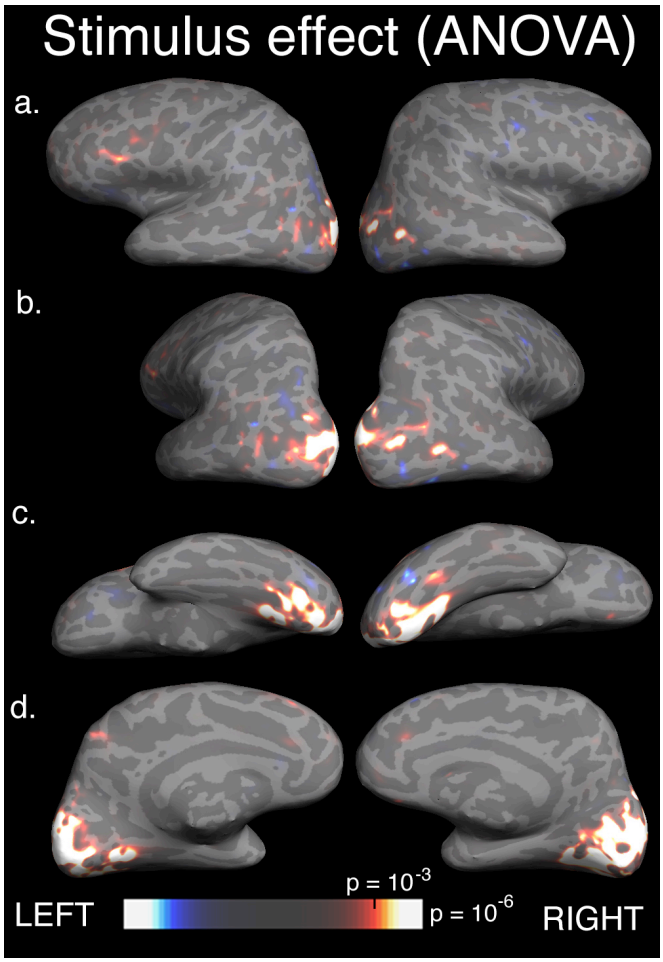

Figure S2. Surface-based group average: Stimulus effect. Here we contrast the Attention + Stimulus condition and the Attention conditions to quantitatively show areas which show significant response to the stimulus differential between the wedge and background. Analysis and display parameters are the same as in Figure S1 except here the red-yellow-white coloring range represents the Stimulus effect.

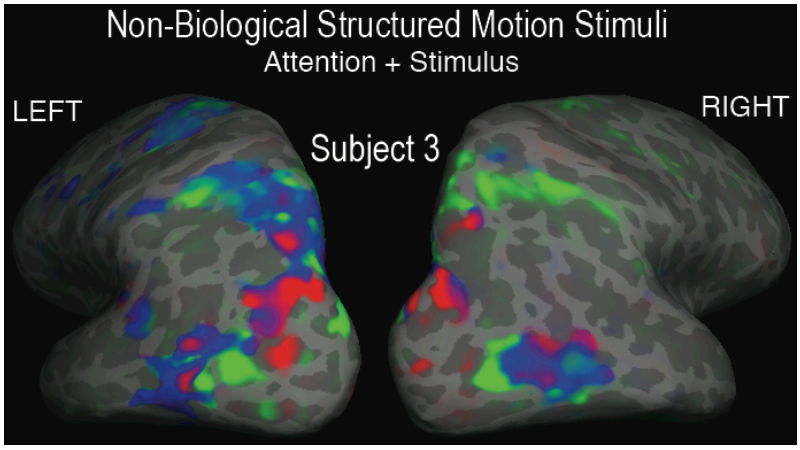

Figure S3. Individual subject data from the version of the experiment where non-biologically moving objects were used instead of point-light biological motion. Visibly saturated phase colors begin to emerge at $p < 10^{-5}$.